DOI: 10.1002/cphc.200700513

Hierarchical Organisation on a Two-Dimensional Supramolecular Network

Paul A. Staniec,[a] Luís M. A. Perdigão,[a] Alex Saywell,[a] Neil R. Champness,[b] and Peter H. Beton*[a]

The spontaneous organisation of molecules into larger structures is pervasive in biological systems and has been identified as a key pathway towards the realisation of "bottom-up" strategies for controlled nanostructure formation.[1,2] A common aspect of organisation in naturally occurring systems is the formation of structures that display hierarchies of order. Currently there are many examples of artificial self-assembled molecular nanostructures which display a single level of order. The extension of organisation in this class of materials to hierarchies of order provides a challenge which has recently attracted considerable interest.[3] This is of particular relevance to spontaneous organisation on surfaces,[2,4–25] a rapidly developing research field with great promise for applications such as biosensors and molecular electronics. Example of hierarchical organisation of molecular clusters was recently demonstrated by Blüm et al.[4] and Spillmann et al.[5] In addition, several examples of systems which display multiple levels of organisation have been realised through an interplay of molecular self-assembly and a second physical ordering mechanism arising from, for example, surface reconstruction[8,13,17,26,27] or dewetting.[28]

Herein we show that hierarchies of organisation may be introduced intrinsically by a self-assembled two-dimensional network. Specifically, we show that a self-assembled template can be used, not only to stabilise size-specific molecular nanostructures, but also influence their relative placement. The system reported here is a new intermixed bi-molecular structure formed by perylene tetra-carboxylic di-imide (PTCDI) and melamine on Au(111) in which rows of pores are formed, each of which has the capacity to stabilise a C_{60} dimer. Importantly, we observe a non-random pore occupancy with an enhanced probability of filling for nearest neighbour sites along the rows. These results imply that the supramolecular network imposes a hierarchy of organisation. At the lowest level of order the network cavities provide size-controlled capture sites for highly specific cluster geometries, while on a larger scale a correlation of occupancy is promoted within the network.

[a] P. A. Staniec, Dr. L. M. A. Perdigão, A. Saywell, Prof. P. H. Beton
School of Physics & Astronomy
University of Nottingham
Nottingham, NG7 2RD (U.K.)
Fax: (+44) 115-951-5180
E-mail: Peter.Beton@nottingham.ac.uk

[b] Prof. N. R. Champness
School of Chemistry, University of Nottingham
Nottingham, NG7 2RD (U.K.)

A Au(111) surface was prepared by loading a 5 mm × 10 mm piece of gold on mica (purchased from Molecular Imaging Inc.) into a UHV system with a base pressure of 1×10^{-10} torr. The surface was cleaned using Ar ion sputtering (4×10^{-6} torr, 1 kV, 1–3 μA) followed by annealing at 150–450 °C for several hours. Images of the surface were acquired using a scanning tunnelling microscope (STM) housed within the UHV system operating in constant-current mode at room temperature and using electrochemically etched tungsten tips. Following the sputter-anneal cycle, we observed the characteristic $(22\times\sqrt{3})$ herringbone reconstruction of the Au(111) surface.[29] Both PTCDI and C_{60} were sublimed onto the surface with the substrate held at room temperature. Melamine was sublimed with the substrate held either at room temperature or at an elevated temperature of 80–90 °C.

Sequential deposition of PTCDI and melamine (molecular structures are shown in Figures 1a and b) onto the Au(111) surface leads to the formation of an intermixed phase. Subsequent annealing in the range 60–80 °C results in the formation of hexagonal networks.[7] The ordering of closely related molecules has also been reported by other groups recently.[30,31] By annealing at higher temperature, ~90 °C, the hexagonal networks are converted into a parallelogram arrangement (see Figure 2). At the boundary between these two annealing conditions, it is possible for both hexagonal and parallelogram networks (labelled areas α and β in Figure 2a respectively) to coexist. The same result is achieved by depositing melamine onto a PTCDI covered sample, while the substrate was heated. As illustrated in Figure 2b, these parallelogram networks form large ordered domains, generating sizeable arrays of pores.

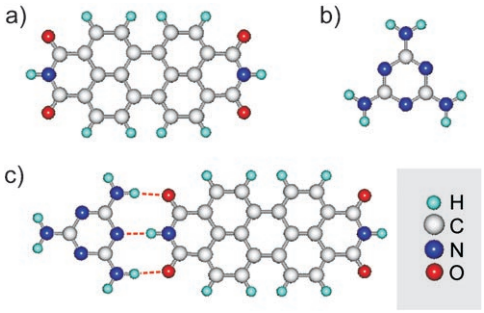

Figure 1. Molecular structure of a) PTCDI and b) melamine. c) The triple hydrogen bond, identified by red dotted lines, between a PTCDI and melamine molecule.

Figure 3a shows an STM image of a small area of a parallelogram network, revealing the molecular arrangement of the structure. As with the hexagonal phase, we are not able to resolve the herringbone reconstruction of the underlying Au(111) surface beneath the network. The stoichiometry of the two bi-molecular phases in Figure 2 is the same, with a melamine:PTCDI ratio of 2:3. The molecular arrangement corresponds to rows (running approximately from bottom right to top left in Figure 3) regularly interlinked by PTCDI molecules. Within the rows there are equal numbers of PTCDI and melamine molecules, with PTCDI molecular pairs in an approximate end-

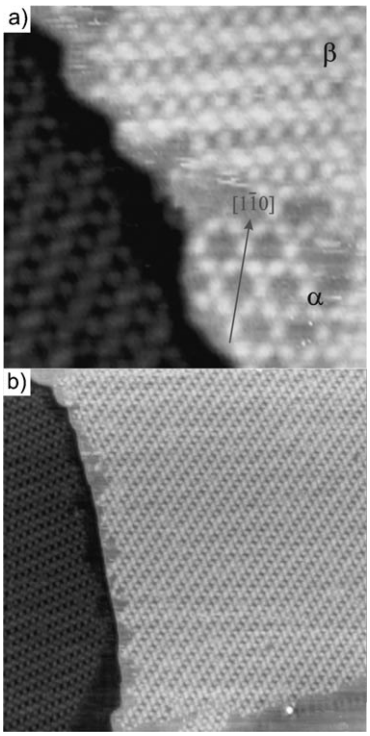

Figure 2. a) STM image of two co-existing bi-molecular phases of PTCDI and melamine on Au(111), 285 Å × 285 Å, −1.8 V, 0.03 nA; the hexagonal and parallelogram phases are labelled as α and β respectively; the [1$\bar{1}$0] direction is identified from the hexagonal network.[6] b) Large area STM image of parallelogram networks, 975 Å × 975 Å, −1.8 V, 0.03 nA.

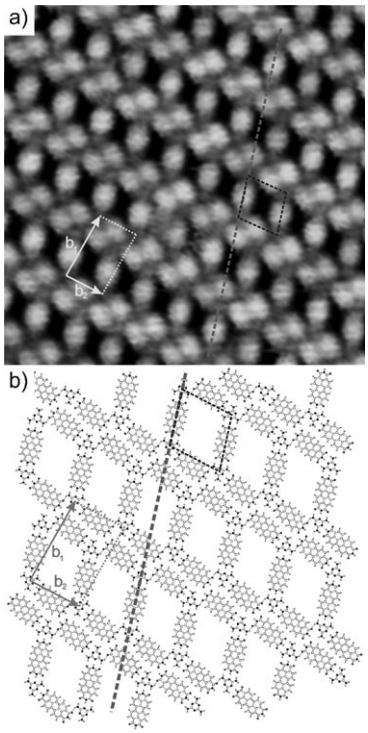

Figure 3. a) Higher resolution STM image, showing the molecular arrangement of a parallelogram network, 175 Å × 175 Å, −1.5 V, 0.03 nA; the direction through alternate pores and along interconnecting PTCDI molecules is highlighted (----- line); the parallelogram nature of the pores is depicted by the dashed box (right); the approximately rectangular unit cell, defined by the unit vectors $\mathbf{b_1}$ and $\mathbf{b_2}$, is also illustrated. b) Schematic of the proposed bi-molecular ordering; the corresponding alternative pore/linking molecule direction, parallelogram pore and unit cell vectors are represented as for (a).

to-end configuration[16] oriented at an angle to the rows. The interlinking PTCDI molecules are aligned at an angle $76.3 \pm 2^\circ$ to the rows as illustrated by the line in Figure 3a. This non-perpendicular alignment leads to the parallelogram shape of the pores, highlighted in Figure 3a. The network unit cell, defined by the unit cell vectors $\mathbf{b_1}$ and $\mathbf{b_2}$ shown on Figure 3a, is approximately rectangular and is measured from our STM images to be $\mathbf{b_1} = 30.7 \pm 0.4$ Å and $\mathbf{b_2} = 19.4 \pm 0.3$ Å, with an internal angle of $87 \pm 2^\circ$. We observe two distinct alignments corresponding to the interlinking PTCDI molecular orientations (green line in Figure 3) either parallel to, or at $17 \pm 2^\circ$ to the $< 1\bar{1}0 >$ directions. The arrangement is chiral and domains of both chiralities have been observed.

We propose a model, shown in Figure 3b, for the observed molecular ordering based upon the internal alignments and unit cell dimensions. The structure is stabilised by triple hydrogen bond junctions (see Figure 1c) between melamine and the interlinking PTCDI molecules. Within the rows, one end of each PTCDI forms a triple hydrogen bond with a melamine and the other end is stabilised by a PTCDI–PTCDI double hydrogen bond as has previously been observed[11,16] and a single hydrogen bond with a melamine molecule. Overall the structure is stabilised by fewer hydrogen bonds than the hexagonal network we have previously reported, although the stoichiometry of the two phases is the same. However, we note that the molecular density is higher in the parallelogram phase. It has recently been shown theoretically[32,33] that the competition between isotropic intermolecular interactions, for example van der Waals interactions, and directional interactions such as hydrogen bonding can lead to the formation of more highly compact surface phases.

We have investigated the potential for the pores in the parallelogram networks to trap sublimed C_{60} molecules, in analogy with previous work.[6,7] In Figure 4a we show STM images acquired following the deposition of ~0.1 monolayers (ML) which clearly show that a number of the parallelogram pores are occupied by C_{60} dimers. A heptameric cluster (labelled α) in an unconverted hexagon is seen on the edge of a parallelogram domain, offering a clear comparison to the dimers. A high resolution image of a filled pore alongside a vacant pore, clearly revealing two individual C_{60} molecules, is shown in Figure 4b. The size-selective stabilisation of the dimer is illustrated in Figure 4c using our proposed model.

Figure 4d shows a large scale image of the surface after the deposition of ~0.1 ML of C_{60}, while Figure 4e shows an array at a coverage of ~0.2 ML. Images such as these give the impression that there is a non-random occupancy of pores and in particular that there is a higher then expected frequency of extended rows of dimers occupying neighbouring pores along the direction highlighted in Figure 4d. We have investigated this effect quantitatively through a statistical analysis of the occupancy of the parallelogram pores for a range of fullerene coverages. Data extracted from a number of images, show a

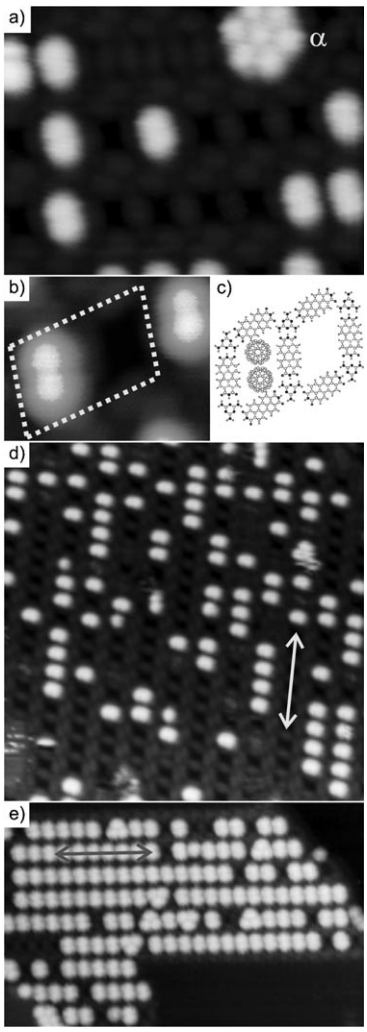

Figure 4. a) STM image of an array of parallelogram pores following a deposition of ≈0.1 monolayers (ML) of C_{60}, 147 Å×110 Å, −2.3 V, 0.03 nA. b) High resolution image of two parallelogram pores, with one pore occupied by a fullerene dimer, 51 Å×41 Å, −1.0 V, 0.03 nA . c) Schematic representation of the two pores highlighted in (b). d) Large area STM image of parallelogram array, illustrating the correlation of captured C_{60} dimers (≈0.1 ML coverage) along the row direction (arrow), 395 Å×395 Å, −1.0 V, 0.03 nA. e) STM image of parallelogram array at a coverage of ≈0.2 ML of C_{60}, 488 Å×305 Å, −2.0 V, 0.03 nA; the correlated row direction is highlighted (arrow).

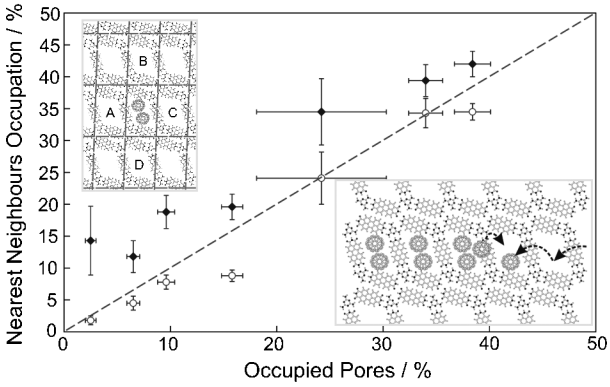

Figure 5. Plot of the fractional occupancy of nearest neighbour site A (or equivalently C) versus average pore occupancy (filled symbols) and occupancy of site B (or equivalently D)—open symbols. Best fit lines to the datasets are also shown together with a line with unit gradient—the systematic observation of occupancy of A/C above this line confirms a correlation in cluster placement. Upper inset shows a schematic of sites A–D; lower inset is a schematic of a kinetic route to growth of cluster-rows.

correlation of pore occupancy, along the row direction. Specifically we have counted the fractional occupation, f_A…,f_D of nearest-neighbour pores A-D (see upper Figure 5 insert). As expected, $f_A \approx f_C$ and $f_B \approx f_D$ within experimental error. We compare this fractional occupation with the average pore occupancy. For example, for a pore occupancy of 9.6±0.8%, the mean nearest-neighbour occupancy, $f_A = 18.8 \pm 2.6$%. This indicates a non-random distribution whereby the formation of chains of dimers along the row direction is correlated, as is apparent in Figure 4d. We summarise our results in Figure 5 where the nearest neighbour occupancy is plotted for coverages up to 50% occupancy and consistently shows non-random statistics. Note that we also plot for comparison the probability of occupancy for the nearest neighbour off-row sites, f_B, where the probability of occupancy is slightly lower than the average pore occupancy. As the coverage is increased and the majority of the pores become occupied, a correlation is observed with respect to the vacant sites. For example, in Figure 4e for which 24.2±6.1% of pores are unoccupied, the fraction of on-row nearest neighbour vacancies (calculated in analogy with f_A) is 34.5±5.2%. The non-random organisation of the placement of fullerene dimers within the network provides clear evidence of a hierarchy of organisation.

We propose a simple model, based on kinetics and shown schematically in the lower inset to Figure 5, which could lead to the growth of rows of occupied pores as observed. The end of the row of occupied pores provides a site with sufficiently high co-ordination to temporarily trap a C_{60} molecule as illustrated in Figure 5 (inset). In this configuration, the molecule is bound to two other C_{60} molecules which, on the basis of simple theoretical arguments[34] leads to an additional stabilisation energy of ≈0.6 eV at this site. We argue that this leads to a high residence time at this site, and acts to mediate dimer formation through the interaction of this temporarily stabilised molecule with a second molecule which hops into the neighbouring cavity (see Figure 5 inset). Thus the probability of dimer nucleation in this pore is enhanced over the average rate of nucleation which is determined by the probability of a random encounter between two freely diffusing molecules.

Finally, we identify interesting aspects of fullerene growth related to the presence of defects in the parallelogram network which can lead to the stabilisation of clusters with more than two fullerenes. Some examples of relevant defects are identified in the STM images shown in Figure 6. Some pores appear occupied by excess PTCDI molecules (labelled α in Figure 6a), observed aligned along either of the diagonals of the pores. These blocked pores are unable to stabilise fullerenes (see Figure 4a). Additionally, 'double pores' (labelled β in Figure 6a) are relatively common through the absence of a single linking PTCDI molecule. These "double pores" still offer size-selective stabilisation of C_{60} clusters, illustrated in Figure 6b, and have been observed containing hexamer clusters (labelled γ,

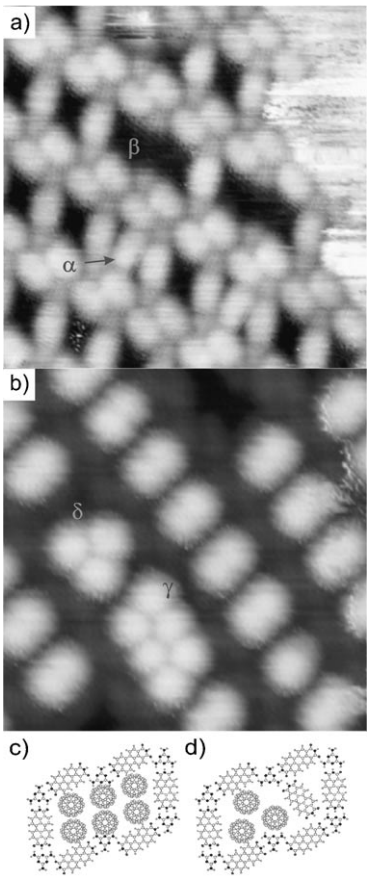

Figure 6. a) STM image illustrating some defects in the parallelogram network, 117 Å×117 Å, −1.5 V, 0.03 nA; a pore blocked by the presence of an excess PTCDI molecule is labelled α; a "double pore" resulting from an absent linking PTCDI molecule is labelled β. b) STM image showing size-selected stabilisation of diverse C_{60} clusters at network defects, 117 Å×117 Å, −2.0 V, 0.03 nA; a hexamer (γ) and trimer (δ) cluster are identified. The stabilisation of hexamer and trimer clusters within the network are schematically demonstrated in (c) and (d), respectively.

Figure 6b). The stabilisation of a hexamer cluster is shown schematically using our proposed model in Figure 6c. In other instances, C_{60} trimers (labelled δ, Figure 6b) have been observed. We attribute these clusters to displaced, but not absent, interlinking PTCDI molecules as shown in Figure 6d.

In conclusion, we have shown the existence of a parallelogram PTCDI–melamine bi-molecular network formed on the Au(111) surface, which forms at a higher annealing temperature to the previously reported hexagonal phase. The network generates large arrays of pores with attractive templating and trapping properties for fullerene clusters. Our key observation is that, in addition to the stabilisation of size specific molecular structures the network also influences the relative placement of clusters leading to a non-random pore occupancy. We argue that this system provides an example of an artificial molecular framework which displays hierarchical surface organisation.

Acknowledgements

We are grateful to the UK Engineering and Physical Sciences Research Council (EPSRC) for financial support under grants GR/S97521/01 and EP/D048761/01.

Keywords: fullerenes · gold · nanostructures · self assembly · surface chemistry

[1] J. V. Barth, G. Costantini, K. Kern, *Nature* **2005**, *437*, 671–679.
[2] S. De Feyter, F. C. De Schryver, *Chem. Soc. Rev.* **2003**, *32*, 139–150.
[3] V. Palermo, P. Samori, *Angew. Chem.* **2007**, *119*, 4510–4514; *Angew. Chem. Int. Ed.* **2007**, *46*, 4428–4432.
[4] M.-C. Blüm, E. Ćavar, M. Pivetta, F. Patthey, W.-D. Schneider, *Angew. Chem.* **2005**, *117*, 5468–5471; *Angew. Chem. Int. Ed.* **2005**, *44*, 5334–5337.
[5] H. Spillmann, A. Dmitriev, N. Lin, P. Messina, J. V. Barth, K. Kern, *J. Am. Chem. Soc.* **2003**, *125*, 10725.
[6] J. A. Theobald, N. S. Oxtoby, M. A. Phillips, N. R. Champness, P. H. Beton, *Nature* **2003**, *424*, 1029–1031.
[7] L. M. A. Perdigão, E. W. Perkins, J. Ma, P. A. Staniec, B. L. Rogers, N. R. Champness, P. H. Beton, *J. Phys. Chem. B* **2006**, *110*, 12539–12542.
[8] M. Böhringer, K. Morgenstern, W.-D. Schneider, R. Berndt, *Angew. Chem.* **1999**, *111*, 832–834; *Angew. Chem. Int. Ed.* **1999**, *38*, 821–823.
[9] J. V. Barth, J. Weckesser, C. Cai, P. Günter, L. Bürgi, O. Jeandupeux, K. Kern, *Angew. Chem.* **2000**, *112*, 1285–1288; *Angew. Chem. Int. Ed.* **2000**, *39*, 1230–1234.
[10] Q. Chen, D. J. Frankel, N. V. Richardson, *Langmuir*, **2002**, *18*, 3219–3225.
[11] D. L. Keeling, N. S. Oxtoby, C. Wilson, M. J. Humphry, N. R. Champness, P. H. Beton, *Nano Lett.* **2003**, *3*, 9–12.
[12] S. Griessl, M. Lackinger, M. Edelwirth, M. Hietschold, W. M. Heckl, *Single Mol.* **2002**, *3*, 25–31.
[13] T. Yokoyama, S. Yokoyama, T. Kamikado, Y. Okuno, S. Mashiko, *Nature* **2001**, *413*, 619–621.
[14] D. Bonifazi, H. Spillmann, A. Kiebele, M. De Wild, P. Seiler, F. Cheng, H.-J. Güntherodt, T. Jung, F. Diederich, *Angew. Chem.* **2004**, *116*, 4863–4867; *Angew. Chem. Int. Ed.* **2004**, *43*, 4759–4763.
[15] S. Stepanow, M. Lingenfelder, A. Dmitriev, H. Spillmann, E. Delvigne, N. Lin, X. Deng, C. Cai, J. V. Barth, K. Kern, *Nat. Mater.* **2004**, *3*, 229–233.
[16] J. C. Swarbrick, J. Ma, J. A. Theobald, N. S. Oxtoby, J. N. O'Shea, N. R. Champness, P. H. Beton, *J. Phys. Chem. B* **2005**, *109*, 12167–12174.
[17] P. A. Staniec, L. M. A. Perdigao, B. L. Rogers, N. R. Champness, P. H. Beton, *J. Phys. Chem. C* **2007**, *111*, 886–893.
[18] D. S. Deak, F. Silly, K. Porfyrakis, M. R. Castell, *J. Am. Chem. Soc.* **2006**, *128*, 13976–13977.
[19] B. Xu, C. Tao, W. G. Cullen, J. E. Reutt-Robey, E. D. Williams, *Nano Lett.* **2005**, *5*, 2207–2211.
[20] M. Stöhr, M. Wahl, C. H. Galka, T. Riehm, T. A. Jung, L. H. Gade, *Angew. Chem.* **2005**, *117*, 7560–7564; *Angew. Chem. Int. Ed.* **2005**, *44*, 7394–7398.
[21] G. Pawin, K. L. Wong, K.-Y. Kwon, L. Bartels, *Science* **2006**, *313*, 961–962.
[22] G.-B. Pan, X.-H. Cheng, S. Höger, W. Freyland, *J. Am. Chem. Soc.* **2006**, *128*, 4218–4219.
[23] E. Mena-Osteritz, P. Bäuerle, *Adv. Mater.* **2006**, *18*, 447–451.
[24] A. Kiebele, D. Bonifazi, F. Cheng, M. Stöhr, F. Diederich, T. Jung, H. Spillmann, *ChemPhysChem* **2006**, *7*, 1462–1470.
[25] H. Spillmann, A. Kiebele, M. Stöhr, T. A. Jung, D. Bonifazi, F. Cheng, F. Diederich, *Adv. Mater.* **2006**, *18*, 275–279.
[26] J. Méndez, R. Caillard, G. Otero, N. Nicoara, J. A. Martín-Gago, *Adv. Mater.* **2006**, *18*, 2048–2052.
[27] S. Clair, S. Pons, H. Brune, K. Kern, J. V. Barth, *Angew. Chem.* **2005**, *117*, 7460–7463; *Angew. Chem. Int. Ed.* **2005**, *44*, 7294–7297.
[28] R. van Hameren, P. Schön, A. M. van Buul, J. Hoogboom, S. V. Lazarenko, J. W. Gerritsen, H. Engelkamp, P. C. M. Christianen, H. A. Heus, J. C. Maan, T. Rasing, S. Speller, A. E. Rowan, J. A. A. W. Elemans, R. J. M. Nolte, *Science* **2006**, *314*, 1433–1436.
[29] J. V. Barth, H. Brune, G. Ertl, R. J. Behm, *Phys. Rev. B* **1990**, *42*, 9307–9318.

[30] M. Ruiz-Osés, N. González-Lakunza, I. Silanes, A. Gourdon, A. Arnau, J. E. Ortega, *J. Phys. Chem. B* **2006**, *110*, 25 573 – 25 577.
[31] M. E. Cañas-Ventura, W. Xiao, D. Wasserfallen, K. Müllen, H. Brune, J. V. Barth, R. Fasel, *Angew. Chem.* **2007**, *119*, 1846 – 1850; *Angew. Chem. Int. Ed.* **2007**, *46*, 1814 – 1818.
[32] J. B. Taylor, P. H. Beton, *Phys. Rev. Lett.* **2006**, *97*, 236102.
[33] V. Burlakov, unpublished results.
[34] L. A. Girifalco, *J. Phys. Chem.* **1992**, *96*, 858 – 861.

Received: July 27, 2007
Published online on September 13, 2007

